

VISCOELASTIC DEFORMATION OF LUNAR BASINS: IMPLICATIONS FOR LUNAR FAR SIDE THERMAL HISTORY BASED ON SELENO DETIC DATA OF KAGUYA. S. Kamata¹, S. Sugita², Y. Abe¹, Y. Ishihara³, Y. Harada³, N. Namiki⁴, T. Iwata⁵, H. Hanada³, and H. Araki³, ¹Dept. of Earth & Planet. Sci., Univ. of Tokyo (7-3-1 Bunkyo, Tokyo, 113-0033, JAPAN; kamata@astrobio.k.u-tokyo.ac.jp), ²Dept. of Comp. Sci. & Eng., Univ. of Tokyo (Kashiwa, Chiba, JAPAN), ³National Astronomical Observatory of Japan (Oshu, Iwate, JAPAN), ⁴Planetary Exploration Research Center, Chiba Institute of Technology (Narashino, Chiba, JAPAN), ⁵Institute of Space and Astronautical Science, Japan Aerospace Exploration Agency (Sagamihara, Kanagawa, JAPAN).

Introduction: The viscoelastic state of the farside of the Moon is very important for understanding pre-mare thermal history of the Moon. Because of the strong dependence of the dynamic viscosity of silicate on temperature, the relaxation state of large-scale topographic relieves may retain the record of the ancient lunar thermal history. In order to extract such record, we developed a new viscoelastic numerical calculation code and compare its results and Kaguya data in this study.

Impact basins are among the most prevailing large-scale topographic features on the Moon and have two modification stages: isostatic compensation and crustal lateral flow. The former process induces rise in topography at Moho and reduces surface topography. In contrast, the latter process reduces both surface and Moho topographies. Since the degrees of progress and the timescales of these processes strongly depend on the viscosity, measured surface topography and estimated Moho topography should provide fundamental information for estimating the temperature of the lunar crust and mantle [1]. However, lunar farside gravity field, which is necessary to estimate farside Moho topography, was not directly measured before Kaguya because of synchronous rotation of the Moon. Consequently, estimations of the lunar viscosity are mostly focused on the nearside. Furthermore, few previous studies take into account elasticity and viscosity simultaneously, although both control the relaxation of topography and internal structure. Also, heat flux, which is proportional to thermal gradient and is one of the most important parameter to constrain the thermal history, has not been explicitly incorporated with viscoelastic models since realistically stratified viscosity profiles require long calculation time.

A lunar observation satellite Kaguya revealed a striking contrast in tectonic state between the nearside and the farside of the Moon. While nearside basins show positive free-air anomaly, farside basins show negative circular free-air anomaly [2]. The latter observation indicates that isostatic compensation has not occurred for these basins and that the farside Moho temperature is relatively low [2]. However, the model used in this temperature estimation is a uniform viscous fluid one. In this study, we investigate the depen-

dences of (1) basin size, (2) heat flux, and (3) crustal thickness on basin relaxation in a Maxwell viscoelastic model and give several constraints on the lunar farside thermal history.

Numerical calculation: In order to take heat flux into account, we applied multilayered Moon models, with 1740 layers with different densities and viscosities. We used a new viscoelastic calculation scheme we developed recently [3]. This method is similar to the initial-value (IV) method [4], which involves both spherical harmonic expansion and time integration. The advantage of our scheme is that the cost of calculation for a multilayered sphere is greatly reduced by using a second-order approximation of the constitutive equation, which allows us to use long time steps without losing the accuracy or stability of the scheme.

Moon model: We assumed 1740 km for the lunar radius, and two-layer Moon (i.e., crust and mantle). The surface density is 2800 kg/m³ and interior density structure is determined by the Adams-Williamson condition. The thicknesses of the crust we consider are 10, 30, 50, 70, and 90 km. The density jump at Moho is determined by the constraint that the surface gravitational acceleration is 1.62 m/s². The bulk (175 GPa) and shear modulus (65 GPa) are assumed to be uniform. Six different values, 10, 20, 30, 40, 50, and 60 mW/m², of surface heat flux are used for our calculations. Here, we consider uniform and time-independent heat flux. The values of thermal conductivity of megaregolith (surface layer with 2km thickness), crust, and mantle are 0.2, 1.5, and 3.0 W/m/K. The temperature at the lunar surface is fixed at 250 K. Based on these values and rheological parameters determined by experiments, temperature and viscosity profiles for each crustal thickness and each heat flux are calculated. In this work, we used dry anorthosite rheology [5] for the crust and dry olivine [6] for the mantle.

Results: Fig. 1 shows typical time evolution of surface and Moho topographies. The initial values are -1 for surface and 0 for Moho topography since both topographies are normalized with initial basin depth. Calculation conditions for this particular case are as follows: the harmonic degree is 4 (the corresponding wavelength is about 2500 km, SP-A diameter), the heat flux is 40 mW/m², and the crustal thickness is 50

km. In this configuration, isostatic compensation occurs within 10^3 yr, and subsequently crustal lateral flow occurs around 10^6 - 10^8 yr. In order to quantify these timescales and the degrees of progress of these processes, we focused on Moho topography and defined a few characteristic variables. The maximum Moho topography during the time evolution is h_{\max} , and the time when the maximum occurs is τ_{\max} . We found the models in which the temperature at Moho is higher than ~ 1400 K exhibit a subsequent decrease in Moho topography. In these cases, h_{\min} and τ_{\min} are defined; the Moho topography reaches its minimum value h_{\min} at the time τ_{\min} . The quantities h_{\max} and τ_{\max} can serve as measures of the degrees of isostatic compensation and the timescale for switching of basin modification stages from isostatic compensation to crustal lateral flow, respectively. In addition, $h_{\text{CLF}} \equiv (h_{\max} - h_{\min})/h_{\max}$ serves as a measure of the degree of crustal lateral flow. Half-life $\tau_{1/2}$ of decay in Moho topography was also calculated using data between τ_{\max} and τ_{\min} .

Fig. 2 illustrates dependence of h_{\max} on heat flux and crustal thickness for harmonic degree of (a) 4 and (b) 19 (the corresponding wavelength is about 560 km, Hertzprung diameter). It is clear that h_{\max} strongly depends on heat flux regardless of harmonic degree. Although crustal thickness dependence is very different for different harmonic degrees, it is weaker than that on heat flux.

We also found that higher harmonic degree, larger heat flux, thicker crust leads to smaller τ_{\max} . In contrast, h_{CLF} and $\tau_{1/2}$ strongly depends on harmonic degree and crustal thickness but only weakly on heat flux; higher harmonic degree or thinner (thicker) crust gives smaller h_{CLF} ($\tau_{1/2}$). In other words, both isostatic compensation and crustal lateral flow occur with shorter timescales for smaller basins. This result is remarkable because uniform viscous layer models predict opposite result. One explanation for this rather puzzling result is that the shear stress for a smaller basin is more concentrated in a shallow, high viscosity, and elastic layer. Consequently, both isostatic compensation and crustal lateral flow is not achieved for smaller basins, results in smaller τ_{\max} , h_{CLF} and $\tau_{1/2}$.

Implications for the lunar farside thermal history: Our calculation results lead to a number of important implications of the lunar thermal history when they are compared with Kaguya's selenodetic data. The very small free-air anomaly in SP-A indicates almost complete isostatic compensation [7]. This observation indicates that the heat flux was large enough to induce a large amount of mantle uplift soon after the ancient formation of SP-A. This places an important constraint on the heat flux of the Moon, for example,

$> 60 \text{ mW/m}^2$ is required for 80% compensation (Fig. 2a). Another observation that smaller farside basins, such as Hertzprung, show little isostatic compensation [2], suggesting that the heat flux was significantly decreased to $\sim 10 \text{ mW/m}^2$ at least at formation ages of these basins (Fig. 2b). In addition, some basins with little Bouguer anomaly and small topographic relief, such as Tranquillitatis on the nearside and Keeler-Heaviside on the farside, may have experienced prominent crustal lateral flow [1]. Enrichment in radioactive element on the nearside and thick crust on the farside may keep the temperature at Moho higher than 1400 K until crustal lateral flow had occurred. Moreover, thicker crust gives smaller τ_{\max} ; rapid onset of crustal lateral flow. Consequently, crustal thinning by gigantic impact of SP-A may played an important role in supporting uplifted mantle until Moho have cooled ($\sim 10^7$ yr for 30 km crust).

References: [1] Solomon S. C. et al. (1982) *JGR*, 87, 3975-3992. [2] Namiki N. et al. (2009) *Science*, 323, 900-905. [3] Kamata S. et al. (2009) *Proc. 42th ISAS Lunar and Planet. Symp.*, in press. [4] Hanyk L. et al. (1995) *GRL*, 22, 1285-1288. [5] Rybacki E. and Dresen G. (2000) *JGR*, 105, 26017-26036. [6] Korenaga J. and Karato S. (2008) *JGR*, 113, B02403, doi:10.1029/2007JB005100. [7] Zuber M. T. et al. (1994) *Science*, 266, 1839-1843.

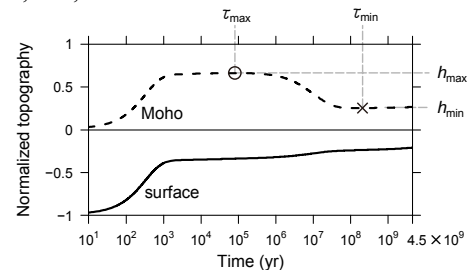


Figure 1. The time evolution of surface and Moho topography normalized with initial basin depth. The solid line and the dashed line represent surface and Moho topography, respectively. The circle and the cross represent the maximum and minimum Moho topography, respectively.

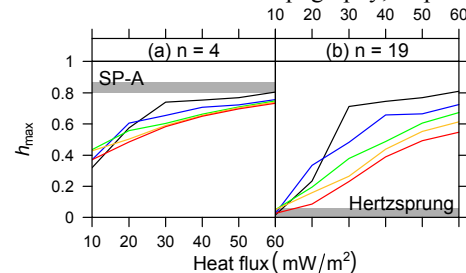


Figure 2. The dependence of maximum Moho topography h_{\max} on heat flux and crustal thickness, for harmonic degree of (a) 4 and (b) 19. The black, blue, green, orange, and red line represent crustal thicknesses of 10, 30, 50, 70, and 90 km, respectively. The shaded zones represent estimated Moho topography using topography and gravity data.